Supporting Information

Super-Resolution Imaging of Photogenerated Charges on CdS/g-C_3N_4 Heterojunctions and its Correlation with Photoactivity

Shuyang Wu, [a] Jinn-Kye Lee, [a] Pei Chong Lim, [a] Rong Xu, [b] Zhengyang Zhang [a,*]

[a] Division of Chemistry and Biological Chemistry, School of Physical and Mathematical Sciences, Nanyang Technological University, 21 Nanyang Link, Singapore 637371.

[b] School of Chemical and Biomedical Engineering, Nanyang Technological University, 62 Nanyang Drive, Singapore 637459.

Corresponding Author

E-mail: zhang.zy@ntu.edu.sg

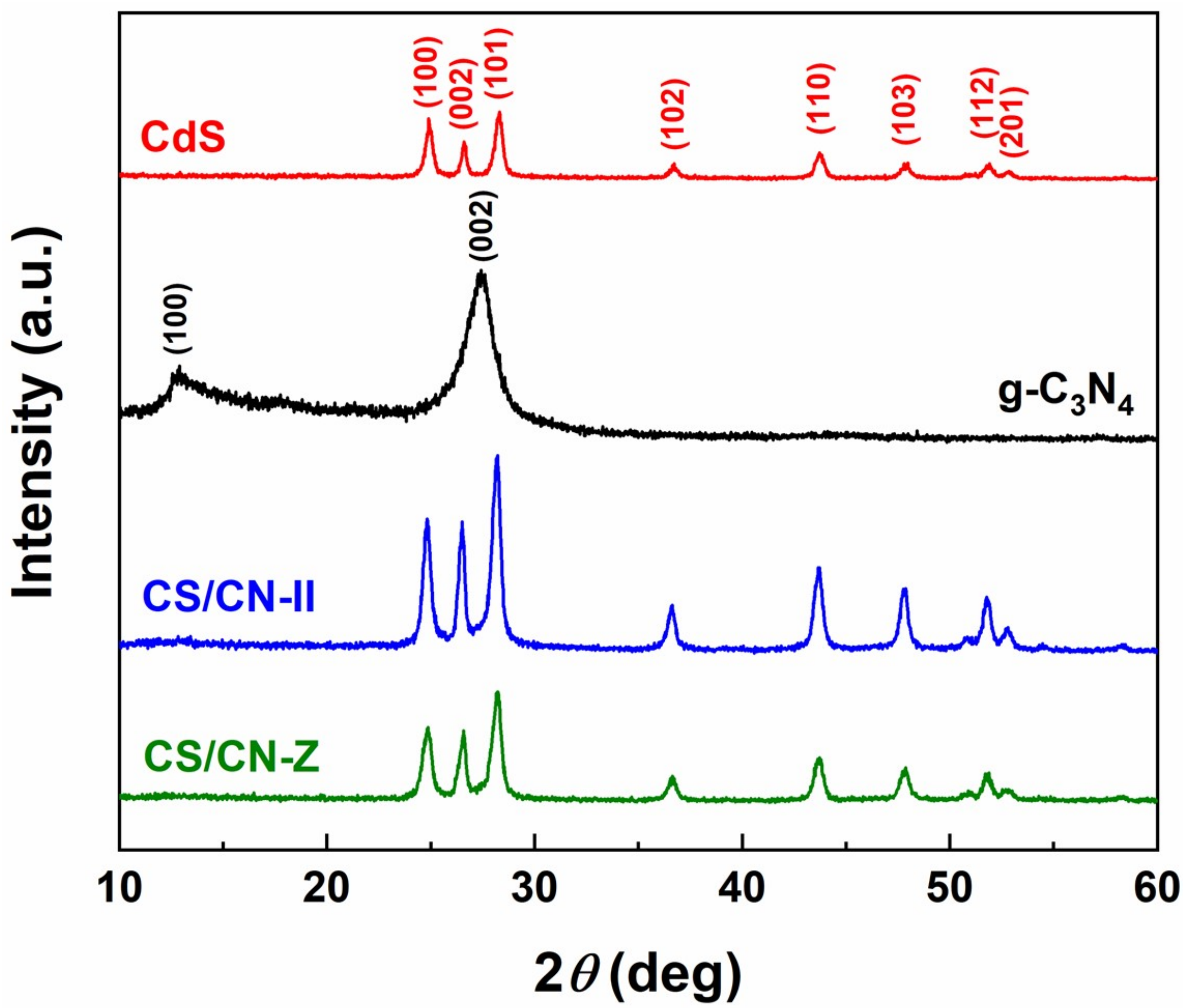

Fig. S1 XRD patterns of CdS, g-C_3N_4, CS/CN-II and CS/CN-Z.

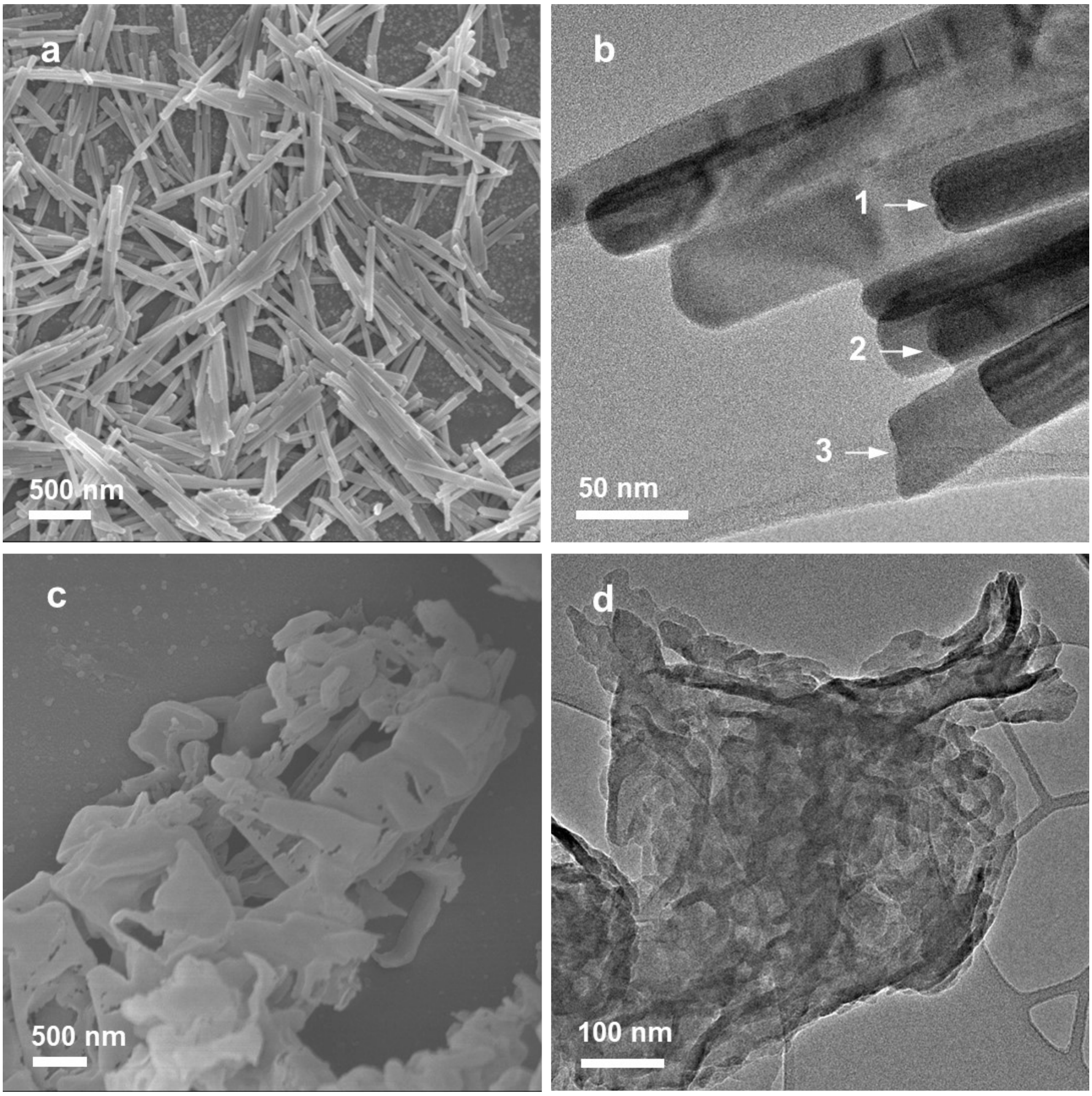

Fig. S2 Morphology of CdS and g-C3N4. FESEM and TEM images of (a, b) CdS and (c, d) g-C_3N_4.

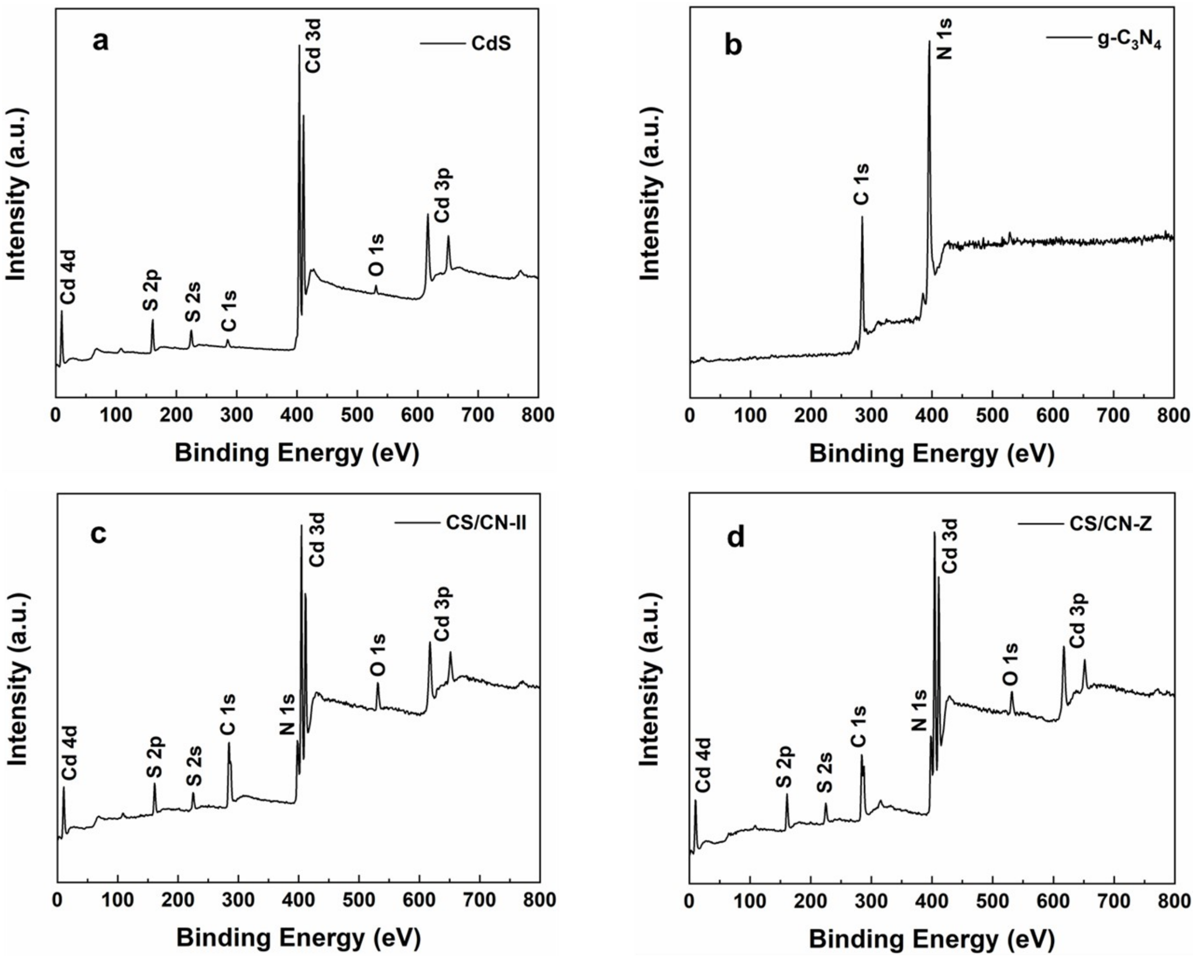

Fig. S3 XPS survey spectra of (a) CdS, (b) g-C_3N_4, (c) CS/CN-II and (d) CS/CN-Z.

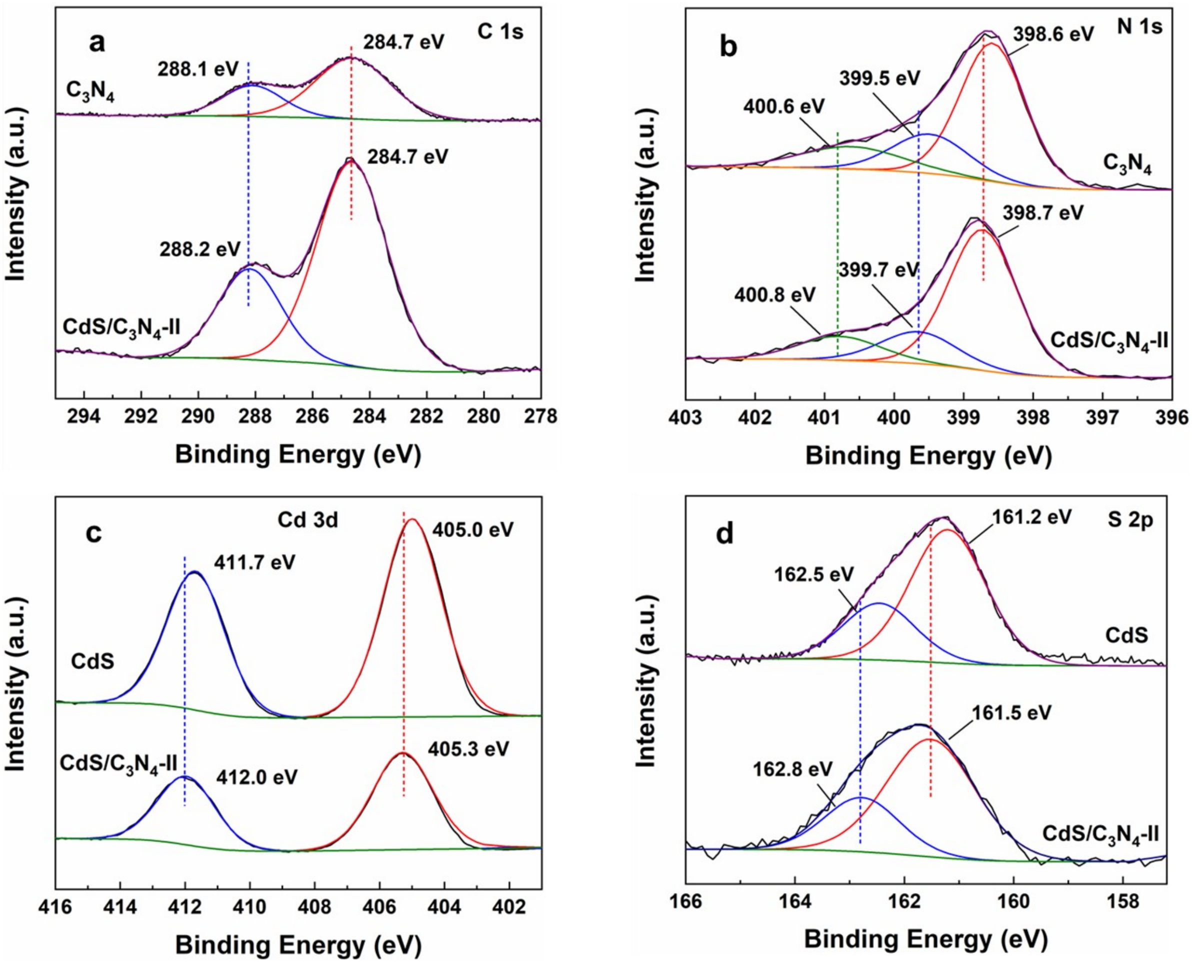

Fig. S4 XPS spectra of (a) C 1s, (b) N 1s, (c) Cd 3d and (d) S 2p for CdS, g-C_3N_4 and CS/CN-II.

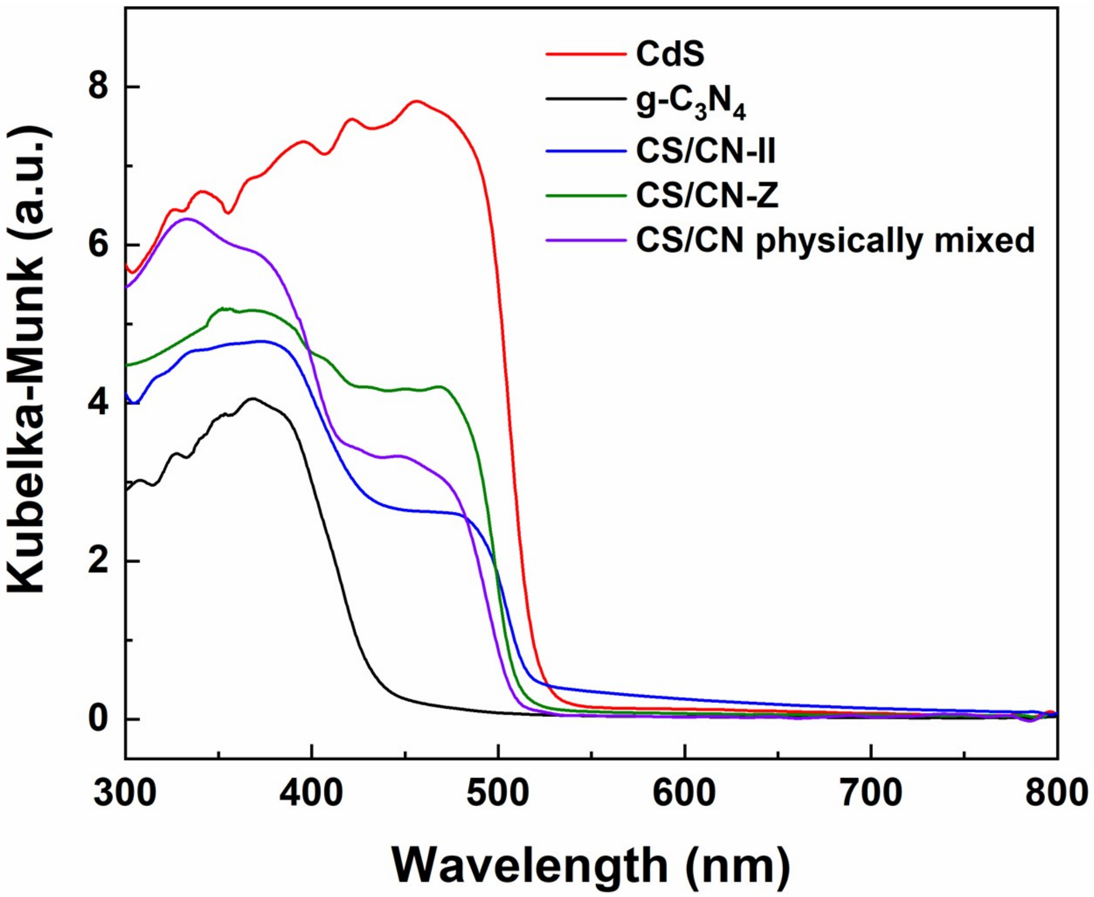

Fig. S5 UV-vis DRS spectra of CdS, g-C_3N_4, CS/CN-II, CS/CN-Z and physically mixed CdS/C_3N_4.

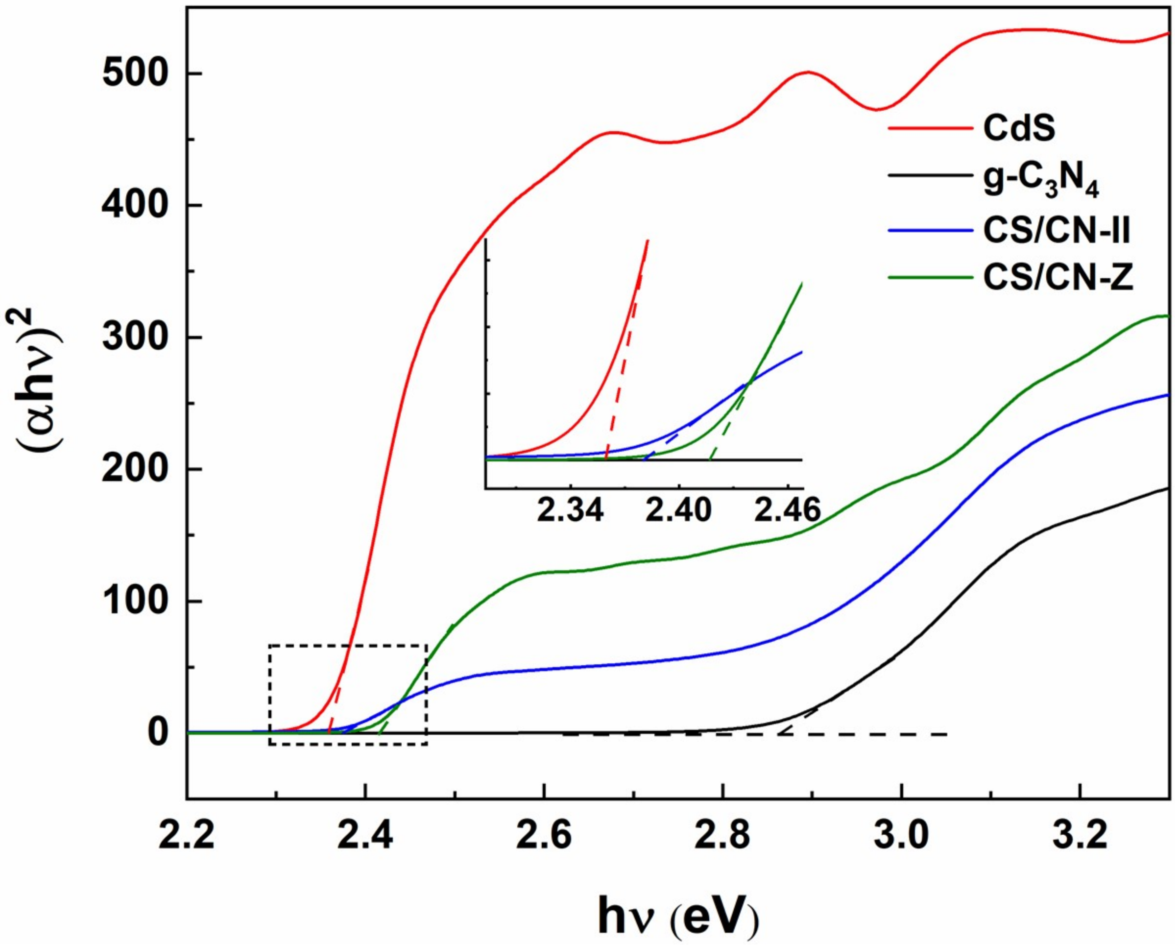

Fig. S6 Tauc plots of as-prepared samples for bandgap analysis.

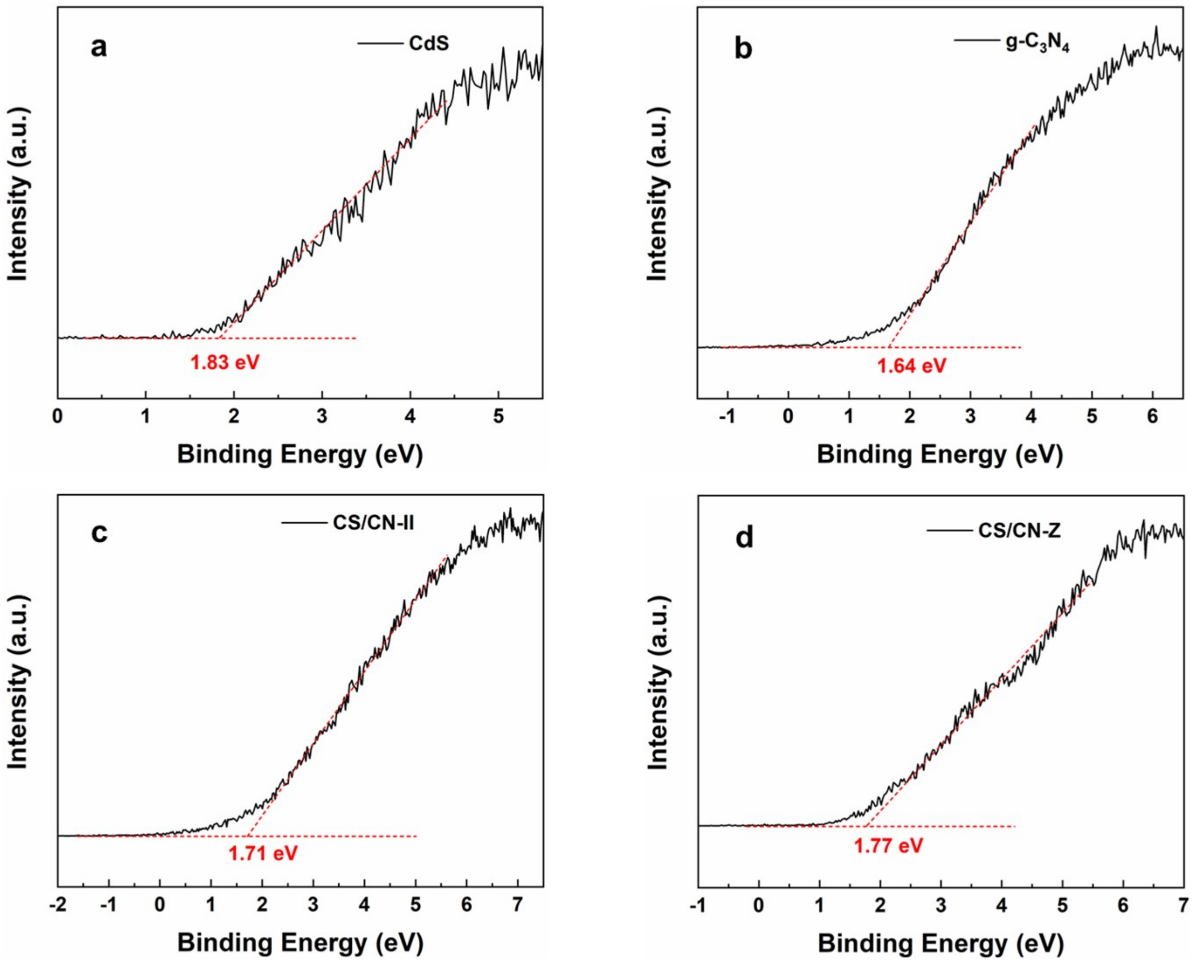

Fig. S7 UPS spectra of (a) CdS, (b) g-C_3N_4, (c) CS/CN-II and (d) CS/CN-Z.

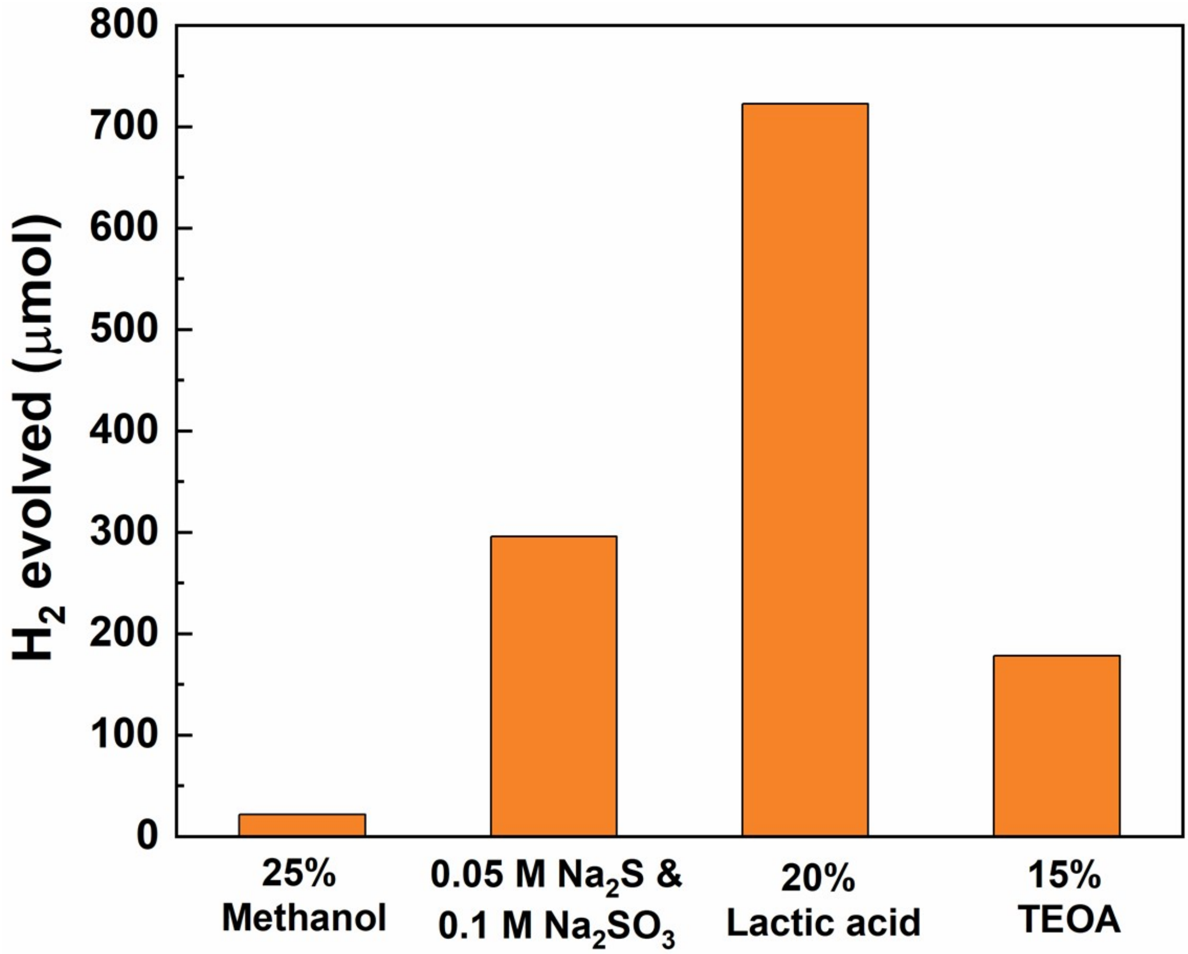

Fig. S8 Photocatalytic H_2 generation for 6 h over CS/CN-II using different sacrificial reagents (50 mg CS/CN-II, 1 wt% Pt, 300 W Xe lamp, > 400 nm).

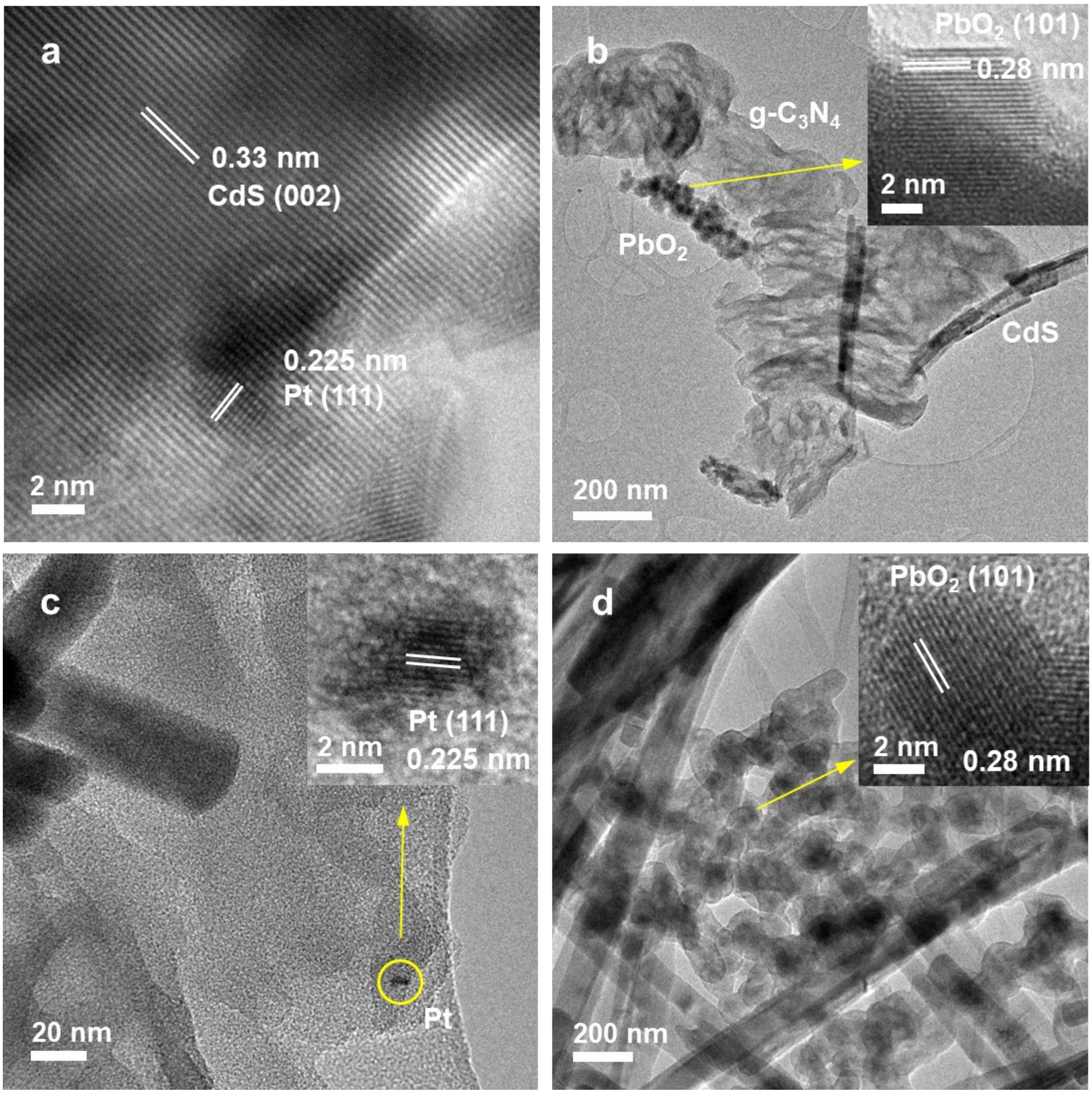

Fig. S9 Charge distribution on CS/CN-II and CS/CN-Z. HRTEM images of CS/CN-II with (a) 1 wt% Pt and (b) 3 wt% PbO_2 loaded, and CS/CN-Z with (c) 1 wt% Pt and (d) 3 wt% PbO_2 loaded. Insets: HRTEM images of the marked positions in the respective images.

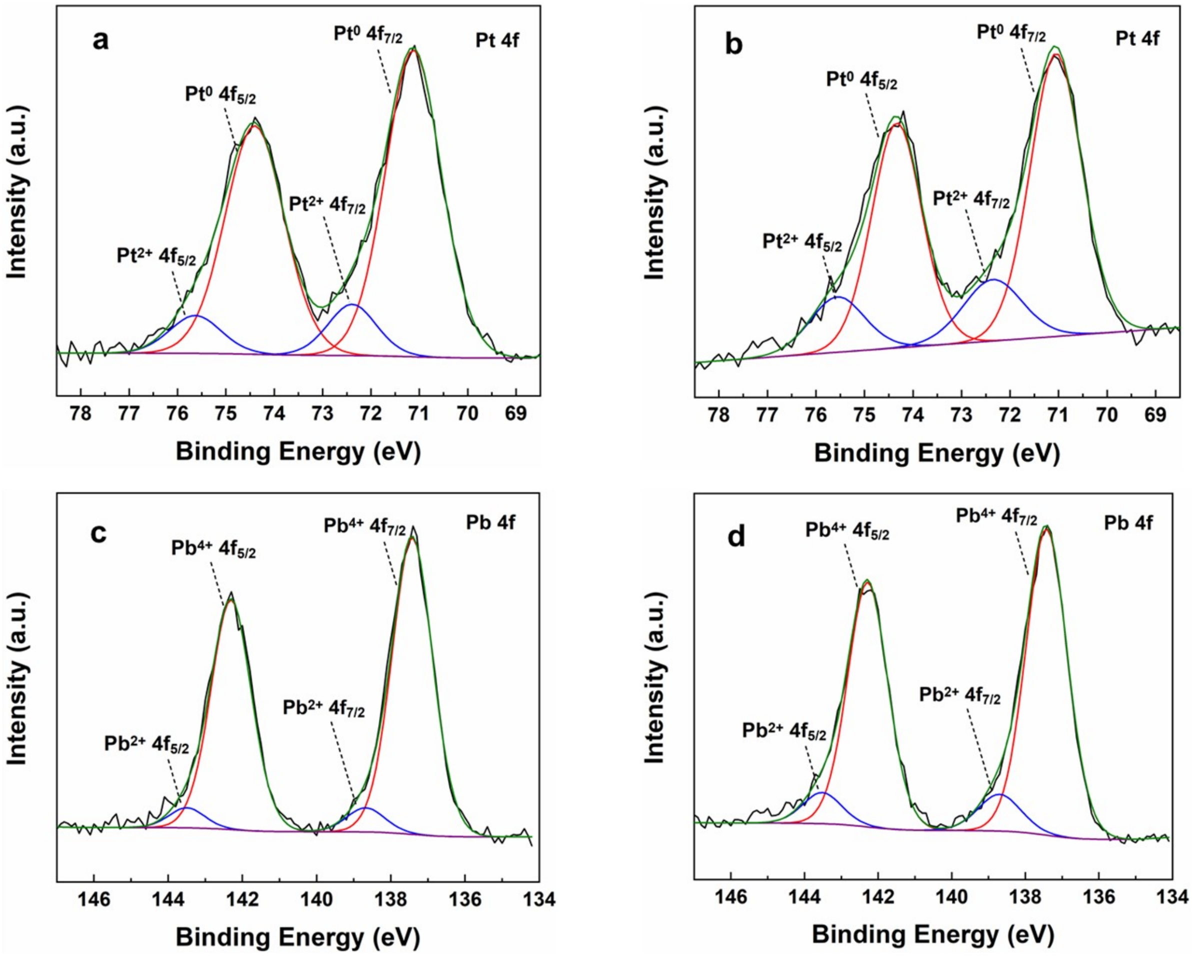

Fig. S10 Percentages of Pt and Pb species after photo-deposition. XPS spectra of Pt 4f in 1 wt% Pt loaded (a) CS/CN-II and (b) CS/CN-Z. XPS spectra of Pb 4f in 3 wt% PbO_2 loaded (a) CS/CN-II and (b) CS/CN-Z.

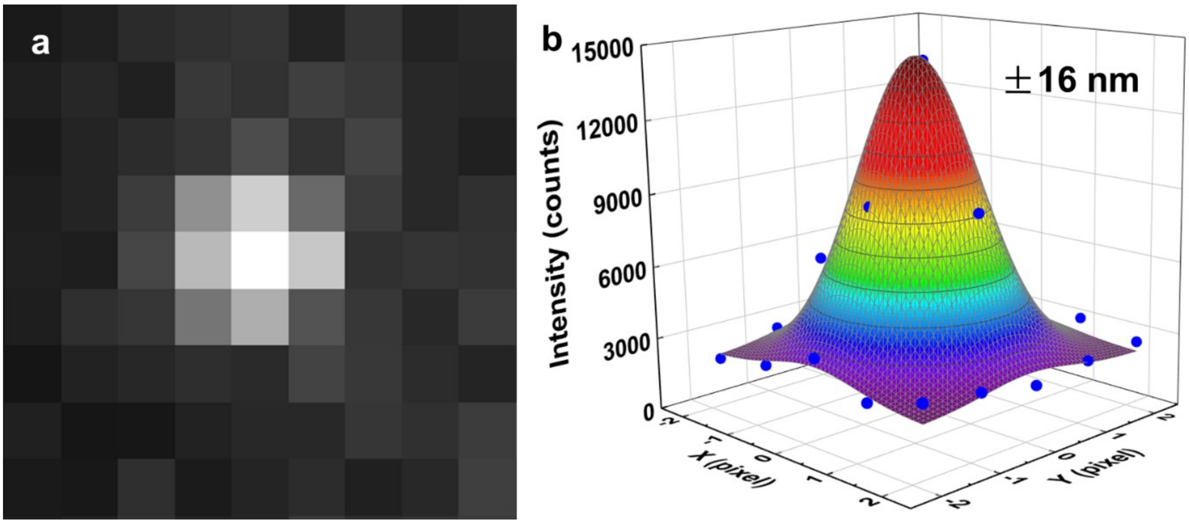

Fig. S11 Localize the center position of single fluorescent molecules with nanometer resolution. (a) Typical fluorescence image of a single resorufin molecule on CdS nanorods under laser excitation. (b) 2D Gaussian fitting of the fluorescence intensity profile with nanometer precision of ± 16 nm.

Fig. S11a is a typical fluorescence image of a single resorufin molecule on CdS nanorods. The fluorescence intensity spreads over a few pixels as a point spread function. Generally, the localization precision can be determined using the method reported in the previous work.[1] As shown in **Fig. S11b**, the center position can be determined by fitting the intensity signals with 2D elliptical Gaussian functions (**Eq. S1**):

$$I\,(x,y) = A + B * exp(-(\frac{(x-x_0)^2}{2S_x^2} + \frac{(y-y_0)^2}{2S_y^2})) \qquad \text{(S1)}$$

where (x_0, y_0) is the center position, A is the background level, B is the peak intensity at (x_0, y_0), S_x and S_y are the standard deviations of the Gaussian distribution along the x- and y-axes, respectively. The localization precision (σ_j, $_{j=x,\,y}$) can be calculated based on the pixel size of the camera, the photons collected and background noise level using **Eq. S2**:

$$\sigma_j = \sqrt{(\frac{S_j^2}{N} + \frac{a^2/12}{N} + \frac{8\pi S_j^4 b^2}{a^2 N^2})} \qquad \text{(S2)}$$

where N is the photons collected, a is the pixel size, and b is the background noise in photons. In the example shown in **Fig. S11**, the parameters are determined to be S_x = 133 nm, S_y = 131 nm, a = 160 nm, N = 612 and b = 16. Thus, σ_x =16 nm and σ_y =15 nm are obtained. The average localization precision is calculated to be σ_{xy} = 16 nm using **Eq. S3**:

$$\sigma_{xy} = (\sigma_x + \sigma_y)/2 \quad \text{(S3)}$$

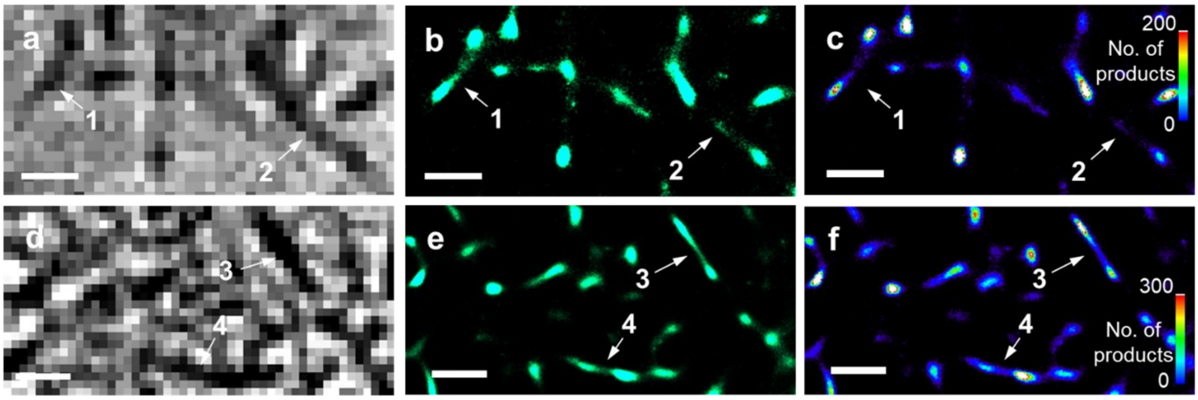

Fig. S12 (a, d) Conventional brightfield images, (b, e) SRM images and (c, f) density maps (bin size: 25 nm × 25 nm) of pure CdS with resazurin. Scale bar: 1 μm.

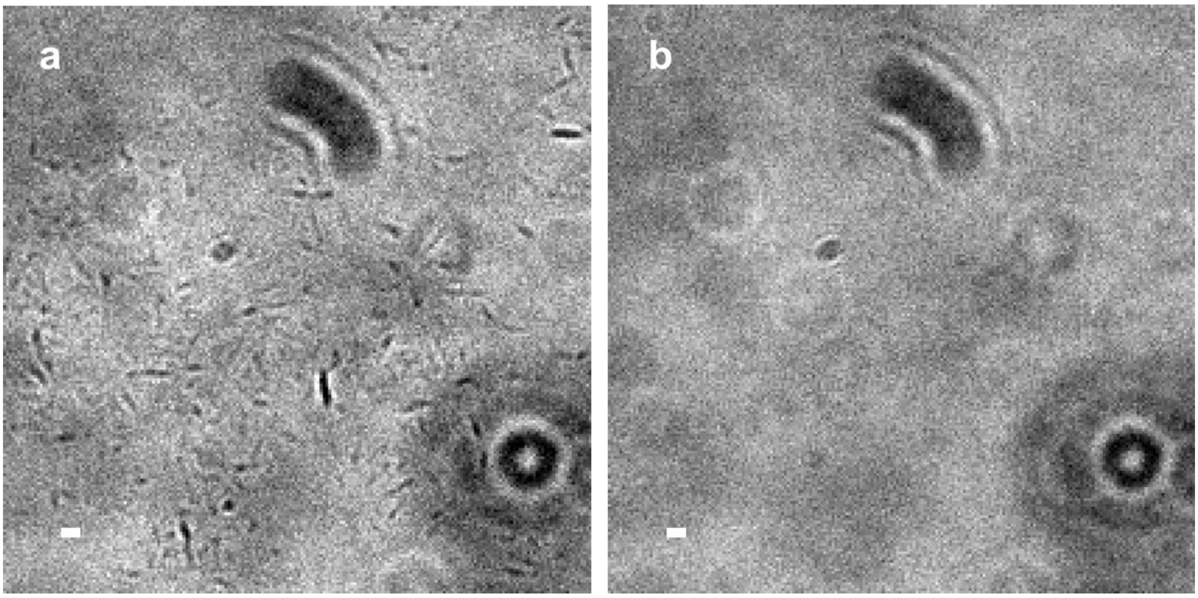

Fig. S13 Conventional brightfield images of pure CdS with amplex red (a) before irridiation and (b) after irradiation. Scale bar: 1 μm.

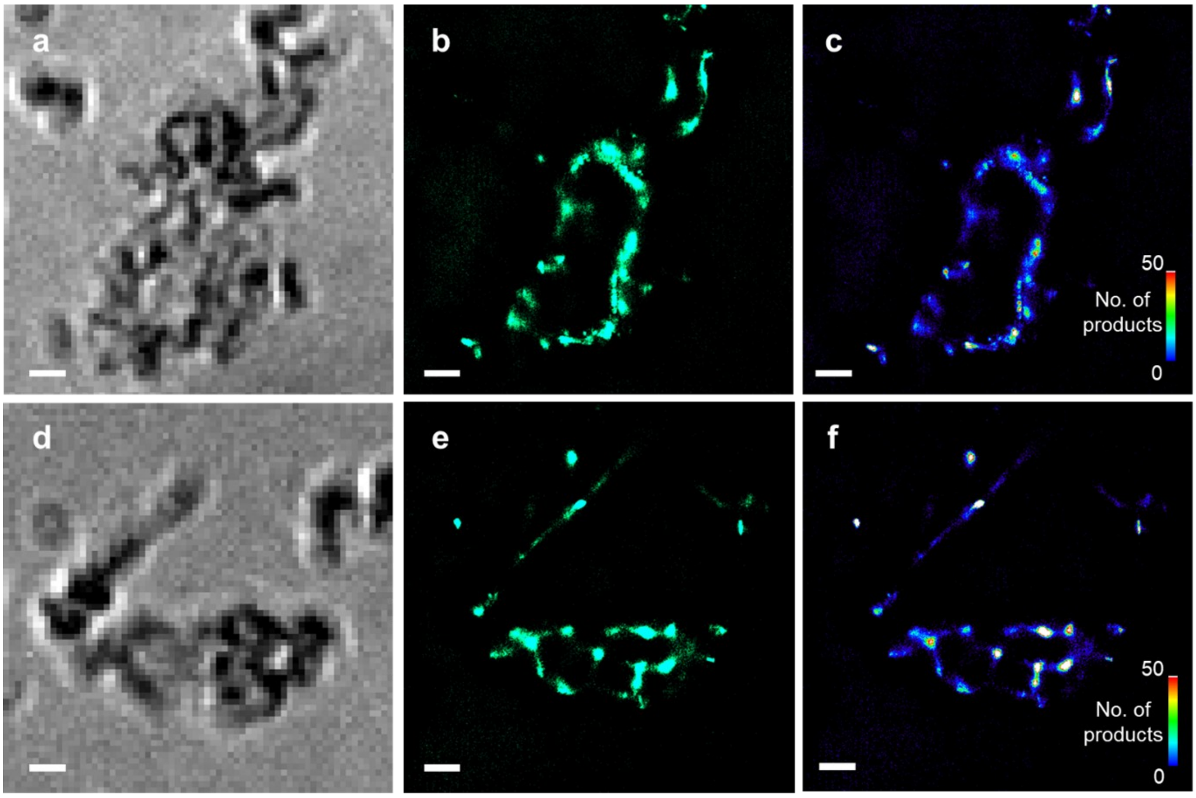

Fig. S14 (a, d) Conventional brightfield images, (b, e) SRM images and (c, f) density maps (bin size: 25 nm × 25 nm) of pure g-C_3N_4 with resazurin. Scale bar: 1 μm.

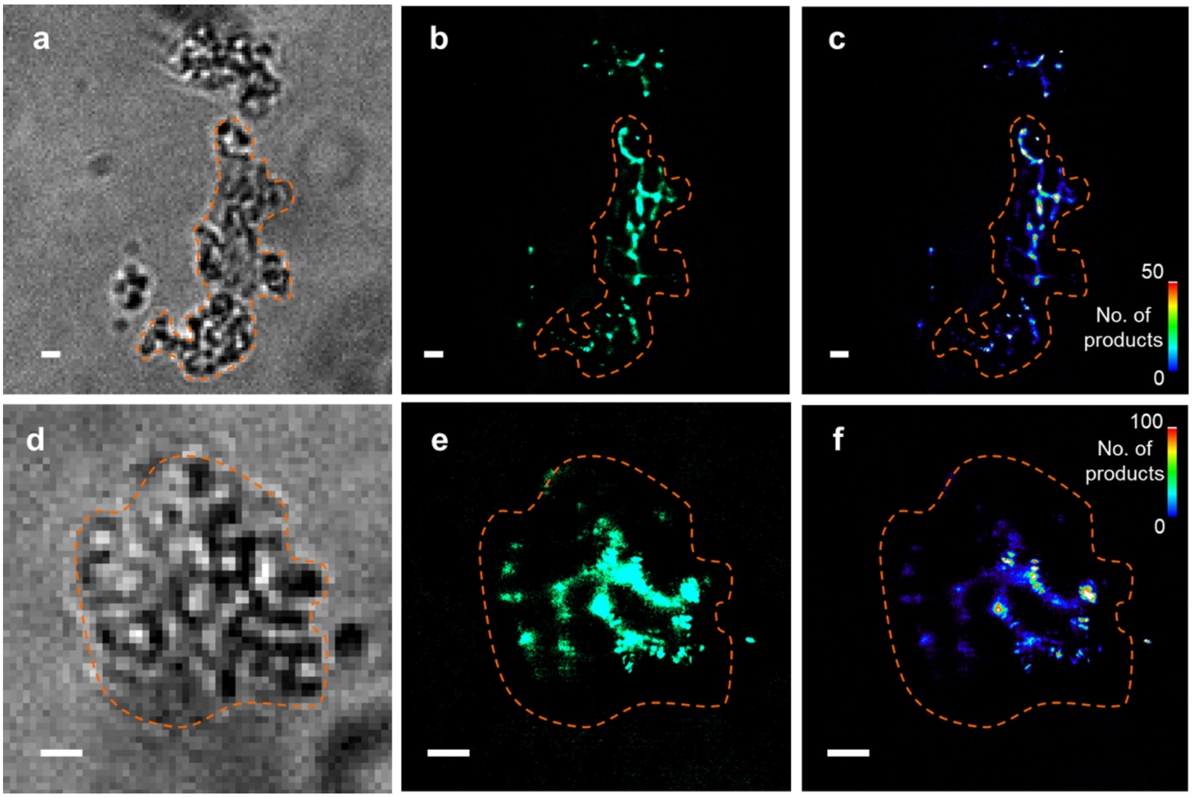

Fig. S15 (a, d) Conventional brightfield images, (b, e) SRM images and (c, f) density maps (bin size: 25 nm × 25 nm) of pure g-C_3N_4 with amplex red (The dashed lines are the outlines of g-C_3N_4 in the brightfield images). Scale bar: 1 μm.

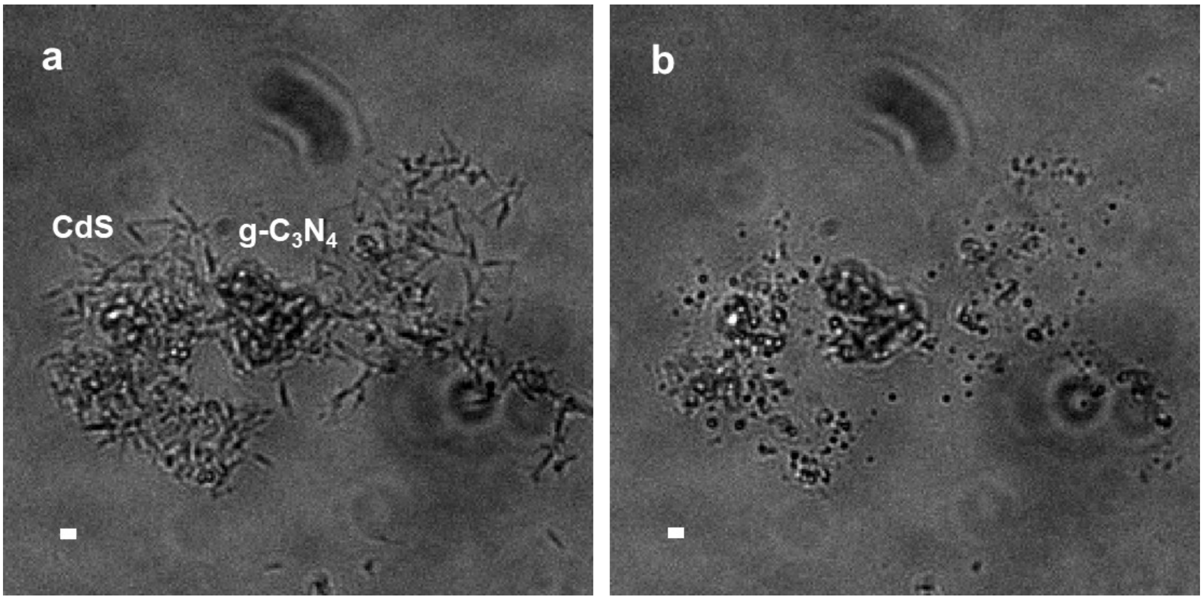

Fig. S16 Conventional brightfield images of CS/CN-Z with amplex red (a) before irridiation and (b) after irradiation. Scale bar: 1 μm.

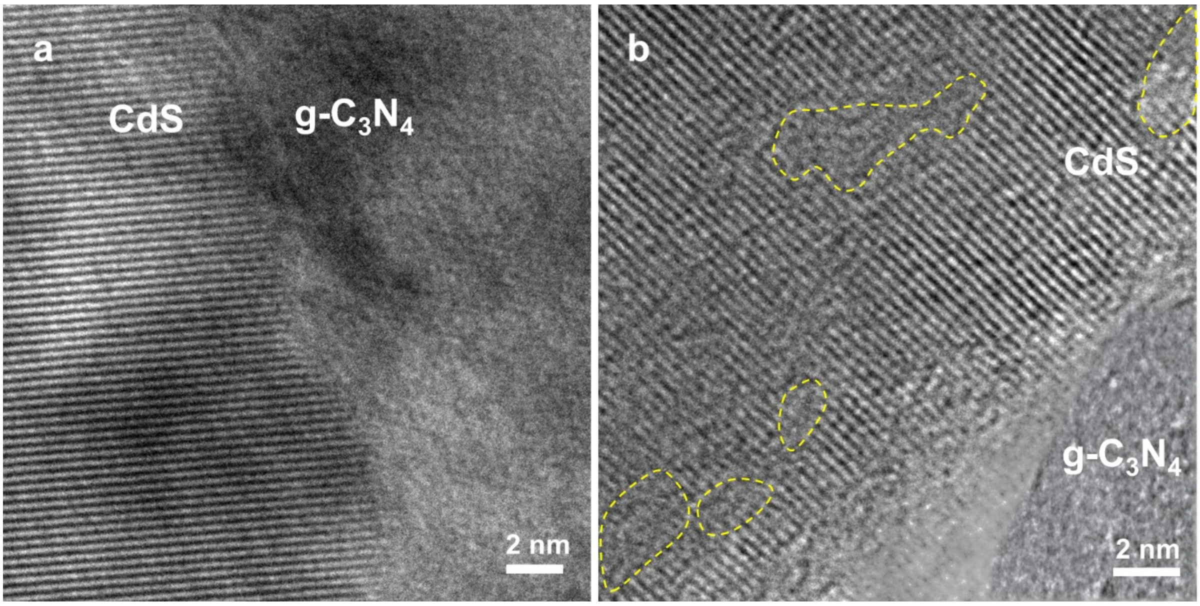

Fig. S17 HRTEM images of (a) CS/CN-II and (b) CS/CN-Z.

Table S1. Summary of typical CdS/g-C_3N_4 composites for photocatalytic H_2 generation.

Reference	Photocatalysts	Catalyst weight	Light source	Cocatalyst	Scavenger	H_2 production rate (μmol h^{-1} g^{-1}), (μmol h^{-1})
This work	CS/CN-II	50 mg	300 W Xe, > 400 nm	1 wt% Pt	20 vol% lactic acid	2410 (120.5)
2	S-doped g-C_3N_4/Au/CdS	100 mg	300 W Xe, > 420 nm	5 wt% Au	20 vol% lactic acid	1060 (106)
3	CdS/g-C_3N_4	50 mg	300 W Xe, > 420 nm	5 wt% Pd	0.5 M Na_2S and 0.5 M Na_2SO_3	293 (14.65)
4	CdS/g-C_3N_4	10 mg	300 W Xe, AM 1.5G	3 wt% Pt	30 vol% TEOA	2240 (22.4)
5	CdS/g-C_3N_4	100 mg	300 W Xe, > 420 nm	3 wt% Pt	10 vol% TEOA	716 (71.6)
6	CdS/g-C_3N_4	50 mg	300 W Xe, > 400 nm	3 wt% Pt	20 vol% TEA	2340 (117)
7	CdS/g-C_3N_4	100 mg	300 W Xe, > 420 nm	2 wt% Pt	0.35 M Na_2S and 1 M Na_2SO_3	2590 (259)
8	$Cd_{0.8}Zn_{0.2}S$/Au /g-C_3N_4	50 mg	300 W Xe, > 400 nm	2 wt% Au	0.1 M glucose	123 (6.15)
9	CdS/g-C_3N_4	50 mg	300 W Xe, > 420 nm	3 wt% Ag	10 vol% lactic acid	1376 (68.8)
10	Cyano groups-C_3N_4/ CdS	30 mg	300 W Xe, > 420 nm	1 wt% Pt	14 vol% lactic acid	1809 (54.3)

Table S2. Pt loading based on ICP measurement and percentages of Pt and Pb species observed from XPS spectra on CS/CN-II and CS/CN-Z after photoreactions.

	1% Pt[a)]			3% PbO_2	
	Pt loading[b)] (Pt^{0} [c)]) (%)	Pt^{0} (%)	Pt^{2+} (%)	Pb^{4+} (%)	Pb^{2+} (%)
CS/CN-II	0.79 (0.69)	87.4	12.6	93.1	6.9
CS/CN-Z	0.71 (0.56)	79.5	20.5	89.0	11.0

[a)] Theoretical loading based on the amount of Pt precursor is 1 wt%; [b)] by IPC measurement; [c)] total Pt% multiply by Pt^{0}% from XPS results.

Reference

1. T.-X. Huang, B. Dong, S. L. Filbrun, A. A. Okmi, X. Cheng, M. Yang, N. Mansour, S. Lei and N. Fang, *Sci. Adv.*, 2021, **7**, eabj4452.

2. W. Li, C. Feng, S. Dai, J. Yue, F. Hua and H. Hou, *Appl. Catal. B: Environ.*, 2015, **168**, 465-471.

3. N. Güy, *Appl. Surf. Sci.*, 2020, **522**, 146442.

4. H. Pang, Y. Jiang, W. Xiao, Y. Ding, C. Lu, Z. Liu, P. Zhang, H. Luo and W. Qin, *J. Alloys Compd.*, 2020, **839**, 155684.

5. B. Chong, L. Chen, D. Han, L. Wang, L. Feng, Q. Li, C. Li and W. Wang, *Chinese J. Catal.*, 2019, **40**, 959-968.

6. K. Wang, X. Wang, H. Pan, Y. Liu, S. Xu and S. Cao, *Int. J. Hydrog. Energy*, 2018, **43**, 91-99.

7. Z. L. Fang, H. F. Rong, L. Y. Zhou and P. Qi, *J. Mater. Sci.*, 2015, **50**, 3057-3064.

8. H. Zhao, X. Ding, B. Zhang, Y. Li and C. Wang, *Sci. Bull.*, 2017, **62**, 602-609.

9. L. Qian, Y. Hou, Z. Yu, M. Li, F. Li, L. Sun, W. Luo and G. Pan, *Mol. Catal.*, 2018, **458**, 43-51.

10. Z. Wang, Z. Wang, X. Zhu, C. Ai, Y. Zeng, W. Shi, X. Zhang, H. Zhang, H. Si and J. Li, *Small*, 2021, 2102699.